Biochimica et Biophysica Acta 1798 (2010) 777–787

Contents lists available at ScienceDirect

Biochimica et Biophysica Acta

journal homepage: www.elsevier.com/locate/bbamem

Review

A nanometer scale optical view on the compartmentalization of cell membranes

Thomas S. van Zanten [a], Alessandra Cambi [b], Maria F. Garcia-Parajo [a,c,*]

[a] BioNanoPhotonics Group, IBEC-Institute for Bioengineering of Catalonia and CIBER-bbn, Baldiri Reixac 15-21, 08028 Barcelona, Spain
[b] Department of Tumor Immunology, Nijmegen Center for Molecular Life Sciences, Radboud University Nijmegen Medical Center, 6500 HB Nijmegen, The Netherlands
[c] ICREA-Institució Catalana de Recerca i Estudis Avançats, 08010 Barcelona, Spain

ARTICLE INFO

Article history:
Received 7 July 2009
Received in revised form 13 September 2009
Accepted 20 September 2009
Available online 2 October 2009

Keywords:
Membrane nanodomain
Lipid raft
Single molecule detection
Near-field scanning optical microscopy
Super-resolution optical microscopy

ABSTRACT

For many years, it was believed that the laws of diffraction set a fundamental limit to the spatial resolution of conventional light microscopy. Major developments, especially in the past few years, have demonstrated that the diffraction barrier can be overcome both in the near- and far-field regime. Together with dynamic measurements, a wealth of new information is now emerging regarding the compartmentalization of cell membranes. In this review we focus on optical methods designed to explore the nanoscale architecture of the cell membrane, with a focal point on near-field optical microscopy (NSOM) as the first developed technique to provide truly optical super-resolution beyond the diffraction limit of light. Several examples illustrate the unique capabilities offered by NSOM and highlight its usefulness on cell membrane studies, complementing the palette of biophysical techniques available nowadays.

Contents

1. Introduction . . . 777
2. The cell membrane: more mosaic than fluid . . . 778
3. Probing the dynamic character of cell membranes . . . 779
4. Super-resolution optical microscopy beyond the diffraction limit. . . . 779
   4.1. Far-field optical nanoscopy. . . . 779
   4.2. Super-resolution near field scanning optical microscopy (NSOM). . . . 781
   4.3. Implementation of NSOM for quantitative bioimaging . . . 781
5. Probing model and cell membrane architectures with near-field optical microscopy . . . 782
   5.1. Model membranes inspected by NSOM . . . 782
   5.2. Cell membrane compartmentalization inspected by NSOM . . . 783
6. Summary and outlook . . . 784
Acknowledgments. . . . 785
References . . . 785

1. Introduction

Our quest towards understanding the structure of biological membranes gained considerable speed in 1971, when the fluid mosaic model was published by Singer and Nicolson [1]. This model describes the plasma membrane as a lipid bilayer, forming a two-dimensional fluid in which the molecules are randomly distributed. In contrast with this hypothesis of simple homogeneous lipid mixing, an ever increasing number of publications appear to confirm that cell membranes are heterogeneously arranged both in the plane of the bilayer and across the two leaflets. This heterogeneity has been evidenced by the spatial and temporal confinement exhibited by proteins and lipids in defined micro- and nanometric scale areas of the membrane [2,3]. Dynamic events like change in mobility or temporal association between lipids and proteins within these microdomains can have direct impact on the biological function of these molecules and therefore on cellular processes like cell activation, antigen presentation and cell–cell interactions.

Although much effort has been directed towards studying the dynamic character of cell membranes using biophysical approaches

* Corresponding author. BioNanoPhotonics Group, IBEC-Institute for Bioengineering of Catalonia, Baldiri Reixac 15-21, 08028 Barcelona, Spain. Tel.: +34 93 4039615; fax: +34 93 4020183.
E-mail address: mgarcia@pcb.ub.es (M.F. Garcia-Parajo).

0005-2736/$ – see front matter © 2009 Elsevier B.V. All rights reserved.
doi:10.1016/j.bbamem.2009.09.012

such as fluorescence recovery after photobleaching (FRAP), fluorescence correlation spectroscopy (FCS) and single particle tracking (SPT) (all of them extensively reviewed by excellent specialists in the field) [4–7], much less is known about the real sizes and topological architecture of these domains. The challenge in these studies is given by the dimensions involved, which are beyond the diffraction limit of light and the high packing density exhibited by lipids and proteins preventing their individual inspection using single molecule techniques. In this review we will focus on optical methods designed to explore the nanoscale organization of the cell membrane, with a special focus on near-field optical microscopy (NSOM) to provide optical super-resolution, not limited by the fluorescence properties of the probes neither by the excitation conditions used. However, one should be aware that recent super-resolution far-field approaches are gaining increasing momentum at present and accordingly they also reviewed to some extent in here. Yet, before discussing the optical methodology, it is worthy to briefly summarize the importance of cell membrane compartmentalization for cellular function and the latest consensus on the field.

2. The cell membrane: more mosaic than fluid

Drawing an integral picture of the cell membrane that reflects its spatial and dynamic complexity is just unrealistic. Nevertheless, one can summarize in a simplified manner, as the scheme shown in Fig. 1, the different domains and confined regions that have been identified so far. One should not be misled by this static picture since in fact large stable domains have not been found in living cells [8]. Indeed, several studies suggest that membrane microdomains are small and highly dynamic, constantly changing in size and composition [9–11].

One of the first structures found in the plasma membrane of eukaryotic cells were caveolae. These small (~60 nm) flask-shaped membrane invaginations consist mainly of the caveolin protein, which binds cholesterol. Caveolae have been implicated in a range of cellular functions, such as cholesterol transport, endocytosis and signal transduction [12].

A second main class of membrane inhomogeneities are lipid rafts. Currently, lipid rafts (or membrane rafts) are defined as "small (10–200 nm), heterogeneous, highly dynamic, sterol- and sphingolipid-enriched domains that compartmentalize cellular processes. Small rafts can sometimes be stabilized to form larger platforms through protein–protein and protein–lipid interactions [13]". Lipid rafts have been shown to play an important role in various biological phenomena, ranging from cell adhesion [14], to pathogen binding [15], endocytosis [16] and immune cell signaling [17]. Also, the importance of lipid rafts in the pathogenesis of a variety of conditions, such as virus infection [18], Alzheimer's and prion diseases as well as systemic lupus erythematosus (reviewed in ref. [19]) has been elucidated. In particular, in these diseases lipid rafts have been shown to promote altered signaling or allow abnormal folding of

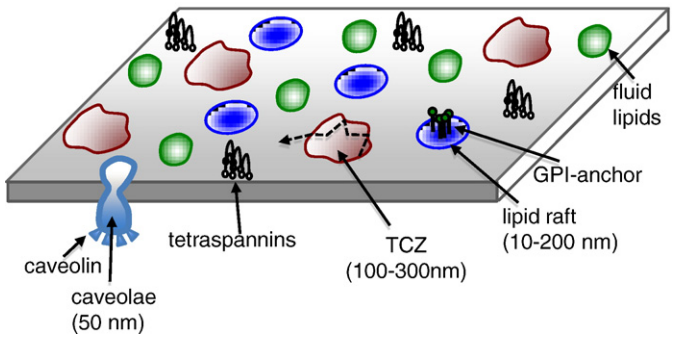

Fig. 1. Schematic and static representation of the various types of microdomains present in the cell membrane.

residing proteins. The involvement of rafts in pathological conditions has further inspired many investigations aimed at unraveling the mechanisms behind the formation of lipid and protein domains, the link between outer and inner leaflet rafts as well as the connection with the cortical actin cytoskeleton.

An example of the dynamic role played by lipid rafts in the reorganization of receptor and signaling molecules is given by the formation of ceramide-enriched membrane domains upon cellular activation. When stimuli such as CD95, CD40, FcγRII, LFA-1, infection with Rhinovirus or UV light treatment occur, rafts are converted into larger membrane platforms by the acid sphingomyelinase, an enzyme that hydrolyses the raft sphingomyelin into ceramide [20]. Ceramide molecules spontaneously aggregate into larger platforms that allow the clustering of receptors and facilitate signal transduction by the recruitment of intracellular signaling components. This indicates that the plasma membrane lipid raft composition is subjected to physiological alterations that subsequently affect cellular signaling events.

In virtue of their lipid anchor, glycosylphosphatidylinositol-anchored proteins (GPI-APs) were among the first molecules to be identified as "official" raft components [10]. Subsequent work from Mayor's group demonstrated that GPI-APs are mainly organized in monomers with a fraction (20–40%) of nanoscale clusters [21]. Interestingly, by using Förster resonance energy transfer (FRET) at the ensemble level, the same group recently demonstrated that the GPI-AP nanocluster fraction tends to spatially concentrate in larger optically resolvable domains and that cortical actin activity affects the formation, dynamics, and spatial organization of these nanoclusters [22]. These studies showed the existence of a steady-state molecular complexation at the nanoscale that is regulated by the cortical actin, implying that a link between outer and inner leaflets must exist.

Membrane compartments are indeed likely to exist both at the outer and at the inner leaflet of the plasma membrane. However, the mechanistic understanding of whether and how outer and inner compartments are linked is still lacking. In signaling T cells, Lasserre and colleagues demonstrated that raft nanodomains are present at both leaflets and that, although sphingolipids and cholesterol are particularly enriched at the outer leaflet, controlled depletion of both these components also affected nanodomain formation at the inner leaflet, suggesting again that a certain degree of leaflet coupling must occur [23]. On the other hand, Wu and coworkers showed large-scale uncoupling of inner and outer leaflet rafts [24]. In fact, by allowing mast cells to adhere onto micrometer-size functionalized patterned lipid bilayers, they did observe that FcεRI clustering induces an actin-dependent co-redistribution of signaling proteins anchored to the inner leaflet, whereas outer leaflet raft components, previously shown to redistribute with IgE-FcεRI crosslinked with soluble ligands, did not show any detectable colocalization with the surface patterned features [24]. Considering the high heterogeneity of membrane nanodomains and their dynamic nature, a possible explanation for this discrepancy could lay in the different membrane receptors, different cell types or different time scales analyzed in these studies.

Besides the lipid–lipid interactions that serve to target proteins to lipid rafts, protein–lipid as well as protein–protein interactions are also important for localizing some proteins to lipid rafts. This is certainly the case for transmembrane proteins, whose association with rafts is still under debate. The transmembrane region may serve to target the proteins to the lipid domains simply based on the length of the transmembrane segment itself [25]. Alternatively, raft-targeting motifs such as palmitoylation can be present in the membrane proximal cytoplasmic region [26,27]. Since palmitoylation can be a transient event, targeting of proteins to rafts can be subject to tight temporal regulation. This phenomenon is well known for the B cell receptor signaling. Palmitoylation of the associated tetraspanin CD81 is required to recruit the B cell receptor to rafts, thus prolonging its signaling in B cells [28]. It should be noted that recent studies have

also demonstrated the formation of plasma membrane microdomains in signaling T cells exclusively created by protein–protein networks and not maintained by interactions with lipid rafts [29]. The diffusional trapping through protein–protein interactions generates microdomains that can recruit or reject specific cell surface proteins during signal transduction.

A third class of domains is characterized by the presence of tetraspanins, a family of integral proteins mainly localized at the plasma membrane and able to interact with one another and with numerous other transmembrane proteins, thereby assembling a network of molecular interactions also called the tetraspanin web [30]. Based on a single-molecule analysis of the tetraspanin CD9, the current view about these membrane domains is that small clusters of tetraspanins, each specifically linked to an interacting molecule, would move within the plasma membrane, often interacting with other domains, either tetraspanin-enriched or lipid rafts, and possibly exchanging some of their components [31]. The association of tetraspanins with integrins is well documented [32,33], although there is still little mechanistic insight into how tetraspanins facilitate integrin-mediated adhesion.

The fourth type of organization discovered in membranes is so-called transient confinement zones (TCZ), which are supposedly formed by a membrane-associated actin mesh network [34]. Indeed, increasing evidence is clearly pointing towards an active role of cortical actin in the formation and dynamics of membrane nanodomains [35]. Interestingly, the diffusion rate of lipids in the plasma membrane is 5–100 times slower than in artificial bilayers, suggesting that long-range interactions between lipids and proteins or lipid and the extracellular matrix may be responsible for this reduction. Kusumi's group has observed the movement of phospholipids at the single-molecule level with a temporal resolution of 25 μs and demonstrated that phospholipids undergo hop diffusion in compartmentalized plasma membranes, proposing the intriguing concept that transmembrane proteins anchored to the actin cytoskeleton meshwork would act as "rows of pickets" to temporarily confine diffusing phospholipids [36]. This has shifted the original paradigm of the plasma membrane as two-dimensional continuum fluid to the new "partitioned fluid," where proteins and lipids diffuse within TCZs [37]. Lenne and colleagues have further substantiated these findings, demonstrating that the cortical actin meshwork and the lipid-based domains are the two main compartmentalizing forces acting in the plasma membrane [38]. More recently, the exact relationship between protein dynamics and actin-defined compartments has been directly visualized [39]. In this elegant paper, the authors not only showed that the FcεRI diffusion is confined within actin-poor areas but also demonstrated that the size and location of these actin barriers changed over time, indicating that the type of diffusion barriers formed by the cytoskeleton is time-dependent [39].

In summary, despite the increasing consensus regarding the fact that biological membranes are compartmentalized both at the lipid and protein level, we still face major challenges in the investigation of the plasma membrane structure. Given the dynamic nature and the nanoscale dimensions of these membrane compartments, techniques that monitor protein and lipid dynamics at high temporal and spatial resolution are needed. Unfortunately, so far, no single technique can combine high spatial resolution (to directly image nanoscale domains) and fast image acquisition (to probe fast dynamics) in one instrument. In here we will focus on techniques that provide optical resolution at the nanoscale and briefly mention the most relevant findings obtained until now using high temporal resolution methods.

3. Probing the dynamic character of cell membranes

The dynamic nature of membrane domains can be investigated via the lateral mobility of fluorescent probes in the cell membrane using FRAP [6,9] or more locally via FCS [7]. In general, these studies revealed that association with lipid rafts is not the dominant factor governing lateral mobility, indicated by the absence of correlation between the diffusion coefficients and characterization as either raft or non-raft marker. In SPT mobility has been investigated by tracking the movement of probes specifically bound to membrane components [40]. As a result of STP experiments, membrane compartmentalization has been widely recognized through the observation of TCZs, regions in the membrane where a protein or lipid is confined much longer than would be expected by simple Brownian motion [37]. TCZs as described in the literature are typically 100–300 nm in size and have lifetimes of hundreds of millisecond to seconds, depending on the experimental sampling rate [34,36,37]. A comprehensive review of the literature on the dynamic aspects of cell membranes micro- and nanodomains is beyond the scope of this paper, and the reader is referred to excellent reviews in the field [4–8,37,40].

4. Super-resolution optical microscopy beyond the diffraction limit

Aside from the dynamic nature of membrane domains, revealing their true size and composition requires high-resolution microscopy techniques. In principle, Förster resonance energy transfer (FRET) is capable of detecting proximity below the optical resolution ($\sim\lambda/2$, where λ is the wavelength of light) since the efficiency of the process depends directly on donor–acceptor distances, typically 1–10 nm [41]. The basis for data interpretation is that clustering stabilizes interparticle distances. FRET efficiencies that are independent of the fluorophore densities have been interpreted as indicative for the existence of clusters [10,41,42]. In addition, FRET experiments do not provide information on distances beyond 10 nm, and thus not able on its own to reveal the true size of domains. It should be noticed that in more recent years, time resolved FRET as combined with fluorescence lifetime imaging (FLIM) and appropriate theoretical modeling is providing more depth-inside in the size of nanodomains in both model systems as well as in living cells, as recently reviewed by Loura et al. [43].

The increased spatial resolution of transmission electron microscopy (TEM) (0.1–10 nm) has been used extensively to visualize a wide variety of protein domains and lipid rafts on the cell membrane. Antibody gold particles of different sizes can be targeted to membrane components revealing their surface distribution [14,15,44–47]. For instance, nanoclustering of the pathogen recognition receptor DC-SIGN on immature dendritic cells [15] and nanodomains of the leukocyte specific integrin LFA-1 at the cell surface of human monocytes [14] have been revealed by TEM. Within the raft field, probably the most intriguing observation has been the absence of co-clustering between two putative raft markers (a GPI-anchored protein and GM1 lipids) [44]. Unfortunately, since TEM requires extensive sample preparation it cannot be extended towards live cell imaging.

High-resolution fluorescence microscopy is compatible with live cell imaging, provides excellent spectral contrast and in combination with sensitive detectors allows the detection of individual molecules. Until only a few years ago, near-field scanning optical microscopy has been the only optical technique able to provide resolution beyond the diffraction limit of light. However, recently developed far-field methods have also demonstrated optical resolution in the nanometer range, not only laterally but also in 3D. Each of the methods is briefly discussed below in terms of their advantages but also limitations. Fig. 2 shows the principles of the four different methods developed so far, with a separation between far-field and near-field approaches.

4.1. Far-field optical nanoscopy

Stimulated emission depletion (STED) microscopy was conceptually introduced more than a decade ago by Hell and colleagues and successfully implemented recently [48–54]. STED creates a nanometric optical region by first exciting fluorophores to an excited state

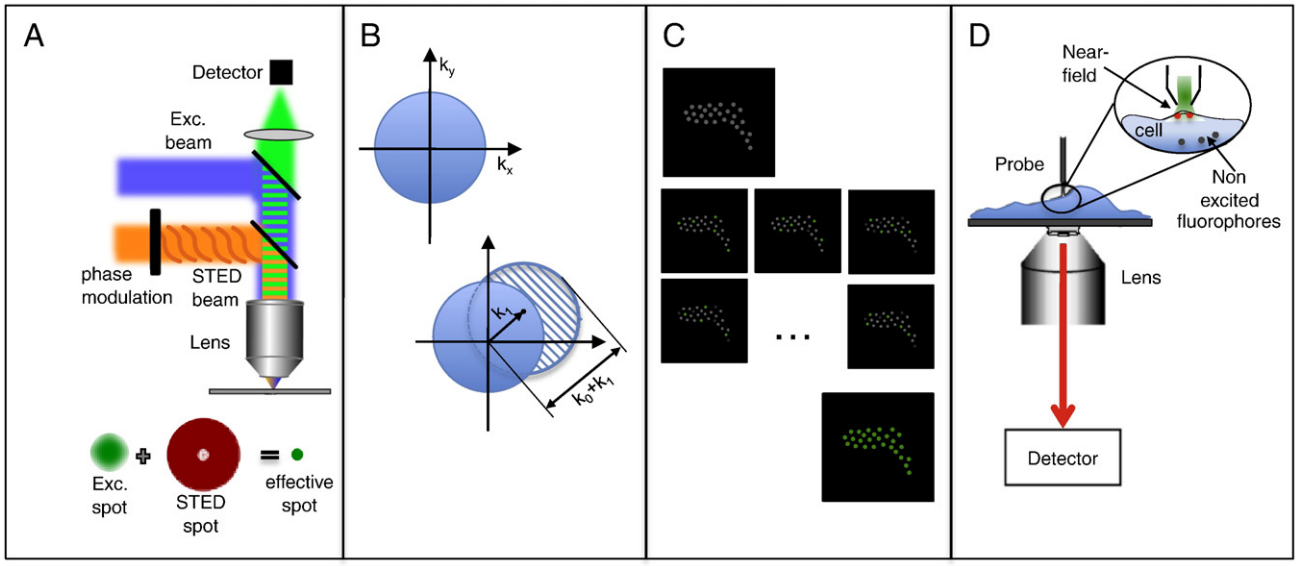

Fig. 2. Different schemes for super-resolution imaging microscopy. (A) Stimulated emission depletion (STED) microscopy, as introduced by Hell's group (adapted from ref. [49]). (B) Structured illumination concept as introduced by Gustafsson. *Top*: Circular observable region of radius k_0 in frequency space observed by a conventional microscope. *Bottom*: New set of information available in the form of moiré fringes (hatched circle) provided that the excitation light contains a spatial frequency k_1. The new region has the same shape as the normal observable region but it is centered at k_1. The maximum spatial frequency that can be detected in this direction is $k_0 + k_1$ (adapted from ref. [54]). (C) Principle of PALM/FPALM and STORM. PALM/FPALM are based on photoactivable autofluorescent proteins while STORM rely on on-off photo switchable organic fluorophores. The techniques use the stochastic photoactivation of single molecules (set to the dark state at the beginning of the experiment as shown in the top panel) and their subsequent nanometric localization over thousands of widefield image frames (series of small panels) to construct a super-resolution image (bottom panel). (D) NSOM uses a subwavelength aperture (~50–100 nm) probe to locally excite the sample surface and to generate point-by-point a super-resolution image related to the size of the probe. Only fluorophores at the cell surface are effectively excited (red dots close to the near-field region) reducing the contribution of background fluorescence from other regions of the cell (dark dots in the interior of the cell).

over a diffraction-limited region using a pulsed laser. A second pulsed laser illuminates the sample with a doughnut-shape like pattern in a wavelength that depletes the excited state of the fluorescent molecules back to the ground state. Fluorescence is effectively detected only from the hole of the doughnut (Fig. 2A). The final spot size can be tuned to balance resolution against signal and imaging speed by controlling the power of the depleting laser, and indeed images with a resolution of ~30 nm have been reported using this technique. However, because of its mere principle, STED requires precise control of the position, phase and amplitude of two laser beams (for single color fluorescence), and its best resolution is restricted to certain dyes able to withstand repeated cycles of excitation and depletion at extremely high intensities. So far, the technique has been mainly applied in neurobiology by the Hell's group, delivering important information on the study of syntaxin clusters and acetylcholine receptors on fixed cultured neurons, as well as to the dynamics of synaptic vesicles over small fields of view at high speeds [50-53]. More recently, STED has been also combined with FCS to observe nanoscale dynamics of membrane lipids and GPI-anchored proteins in living cells [54].

Saturated structured illumination microscopy (SSIM) is conceptually the opposite of STED (Fig. 2B). By using a structured light illumination from two high-intensity power interference beams, most of the fluorescence molecules in the illuminating beams saturate, leaving only small regions unsaturated at the shadows of the interference pattern: the higher the intensity, the smaller the regions [55–58]. The method can be implemented in a widefield (non-scanning) microscope and is capable of high frame rates over wide fields of view. The practical resolving power is determined by the signal-to-noise ratio, which is in turn limited by fluorescence photobleaching. In its linear form, SIM can work at lower intensities reducing photobleaching but can provide only a two-fold resolution increase beyond the diffraction limit. The technique has been applied to study the organization of specific proteins at the neuromuscular junction in *Drosophila* [58] and to elucidate the 3D structure of the nuclear periphery [56].

The two methods described above allow truly optical resolution at the nanometer scale and can be readily extended to 3D imaging. The resolution in fluorescence microscopy can be increased even further by allowing only a subset of fluorescent molecules to be photoactive at a given time and ensuring that the nearest-neighbor distance between active molecules is larger than the diffraction limit. Methods that make use of this principle are photoactivatable localization microscopy (PALM/FPALM) [59,60] and stochastic optical reconstruction microscopy (STORM) [61]. The basic premise of both techniques is to fill the imaging area with many dark fluorophores that can be photoactivated into a fluorescing state by a flash of light. Because photoactivation is stochastic, only a few, well separated molecules "turn on." Then Gaussians are fit to their point spread functions (PSF) to high precision. After the few bright dots photobleach, another flash of the photoactivating light activates random fluorophores again and the PSFs are fit of these different well-spaced objects. This process is repeated many times, building up an image molecule-by-molecule; and because the molecules were localized at different times, the "resolution" of the final image can be much higher than that limited by diffraction (Fig. 2C). The main difference between PALM and STORM resides on the type of fluorophores used for photoactivation: PALM relies on autofluorescent proteins, while STORM uses organic switchable dyes (from the cyanine family). The ascertainable localization accuracy depends strongly on the total number of photons being detected. Especially PALM/FPALM can quantitatively map relative molecular densities with very high localization accuracy over wide fields and in living cells. As already mentioned, these forms of nanoscale image reconstruction methodologies rely on photoswitchable fluorophores, and therefore imaging conditions are consistent with single molecule detection and require so far long acquisition times. PALM/FPALM has been used to reconstruct images of various proteins in thin cellular sections and near the surfaces of whole, fixed cells [59] to study the organization of different proteins within adhesion complexes [62] and to track large populations of single proteins molecules in the plasma membrane of living cells [63–65]. In particular Hess and colleagues exploited the technique to

follow the dynamic distribution of hemagglutinin proteins and discriminate between different raft hypotheses [64]. They observed elongated clusters and irregular domain boundaries suggesting that line tension (and thus lipid fluid phase behavior) plays a limited role in domain shape and proposed that interactions between the cytoskeleton and membrane proteins could produce such irregular cluster size distribution in accordance to previous work from Kusumi and Vale's groups [36,37,29].

With the rapid and widespread implementation of different forms of photoswitchable super-resolution optical microscopy, including multicolor [62,66] and 3D capabilities [67–70], one word of caution should be drawn to the biological community. In fact, several researchers in the field have already highlighted some of the caveats inherent to the approach [71,72]. They include cellular autofluorescence or fluorescence from unactivated fluorophores that obscure the signal from individual molecules, making sparsely labeled structures difficult to image, and photodamage induced by the ultraviolet laser used for photoswitching in PALM/FPALM that can limit its application in live cell imaging. Most importantly, there are also fluorescence related problems such as over-expression, artifactual aggregation, mistargeting or probe specificity that can complicate the interpretation of the images. Indeed, as stated by a recent review in the field: "One of the frustrations of super-resolution microscopy is that it is easy to get images, yet extremely difficult to get biologically meaningful ones. As the novelty of super-resolution microscopy wears off, and the focus shifts to its biological application, it will become increasingly important to adopt careful controls such as correlative and/or simultaneous diffraction-limited imaging to insure that the results are physiologically relevant [72]".

4.2. Super-resolution near field scanning optical microscopy (NSOM)

In far-field optical microscopy, the diffraction limit implies that the minimum distance Δx required to resolve independently two distinct objects is dependent on the wavelength λ of the light used to observe the specimen, and by the condenser and objective lens system, through their refractive indices n and angle of acceptance α, such that $\Delta x = 1/2n \sin\alpha$. This implies that Δx exceeds 300 nm in the case of visible light. When an object, such as microscopic specimen, is illuminated with a monochromatic plane wave, the transmitted or reflected light is collected by a lens and projected onto a detector to form the image. Usually, for convenience and practicality, the detector is placed in the far-field, so that the far-field component of the light, which propagates in an unconfined way, is the only component used to generate the image. On the other hand, the interaction between the imaging light and the specimen also generates a near-field component, which consists of a non-propagating (evanescent) field existing only near the object at distances less than the wavelength of the light. Because the near-field decays exponentially within a distance less than the wavelength, usually it cannot be collected by the lens, thus, it is not detected. This effect leads to the well-known Abbé's diffraction limit. By detecting the near-field component before it undergoes diffraction, NSOM allows non-diffraction limited high-resolution optical imaging. This is achieved in NSOM by placing a probe tip in close proximity to the sample in order to illuminate and/or detect in the near-field. Thus, in NSOM microscopes, the resolution Δx no longer depends on λ but instead on the aperture diameter of the probe (typically between 50 and 100 nm). In contrast to the previously described super-resolution techniques that are restricted to fluorescence and rely on the photophysical properties of the probes used, NSOM can exploit many other optical contrast mechanisms (i.e., absorption, polarization and spectroscopy) in addition to fluorescence.

In its most commonly implemented mode, a subwavelength aperture probe is scanned in close proximity (<10 nm) to the specimen under study (Fig. 2D) to generate an image. Using the probe as a near-field excitation source, the interaction with the sample surface induces changes in the far-field radiation, which is collected in the far field by conventional optics and directed to highly sensitive detectors to provide an optical image [73–76]. An independent mechanism is used to control the distance separation between the tip and the sample and to simultaneously generate a topographic image [77,78]. In this way, a singular feature pertaining to NSOM is produced: correlative optical and topographical imaging with a spatial resolution determined by the probe configuration. Another unique characteristic of near-field excitation is given by the finite size of the probe itself: decreasing the area of illumination obviously reduces the interaction volume and background scatter, which is of major importance in enhancing the sensitivity for spectroscopic applications (fluorescence, Raman, etc.).

Instead of using the probe to illuminate the sample, one can employ far field optics to illuminate the sample and use the probe to collect the evanescent field in close proximity to the sample surface. Although perfectly suitable for some photonic applications [79], its use in fluorescence imaging is less appropriate since far field illumination translates in unnecessary sample photobleaching. A different experimental strategy to NSOM is based on the use of metallic tips, known in the literature as apertureless NSOM [80] when the tip is used as passive scatterer, or tip-enhanced NSOM when the metallic tip is excited to enhance the electromagnetic field at the end of the tip apex [81]. In both cases, the sample is illuminated in the far-field and a metal probe is placed in the tight focus of the illumination beam. The local interaction with the sample surface is subsequently detected as a modulation in the scattered far field. Extreme sensitivity is required to observe the weakly scattered light from the nanometer-sized tip in the presence of the light scattered by the sample. When combined with fluorescence, and the tip is properly excited with radial fields along the tip axis, optical resolutions in the order to 30 nm can be achieved [82–84]. This method is however accompanied by a large fluorescence background generated from far field illumination of the sample, requiring therefore modulation techniques to recover the high-resolution signal [85]. On the positive side of the balance, this method is free from the associated practical difficulties of fabricating circular apertures.

4.3. Implementation of NSOM for quantitative bioimaging

For biological applications, the most widely used configuration is an aperture-type NSOM, incorporated into an inverted optical microscope, with near-field excitation and far-field detection (see Fig. 3). This scheme preserves most of the conventional imaging modes (confocal microscopy for instance), which remain available in combination with the near-field approach. Light that is emitted by the aperture locally interacts with the sample. It may be absorbed, phase shifted, or used to locally excite fluorescent markers, depending on the sample and the contrast mechanisms employed. In any case, light emerging from the imaging zone must be collected with the highest possible efficiency. For this purpose, high NA (oil immersion) microscope objectives are usually employed. The collected light is directed to sensitive detectors, such as avalanche photo-diodes (APD) or photo-multiplier tubes (PMT), via suitable dichroic mirrors for spectral splitting or through a polarizing beam splitter cube for polarization detection. Filters are also commonly used to select the spectral regions of interest removing unwanted spectral components, and inverted optical microscopes are an advantageous solution for light collection, redistribution, and filtering.

In Fig. 3, the excitation light from one or more laser sources is coupled into the optical fiber. The tip is maintained in the near-field of the specimen by the feedback system operating in close loop that precisely controls the separation between the probe and the sample. In addition, a 3D scanner is employed to control the relative positioning of sample and probe. Depending upon design and applications, in principle the scanner may either move the specimen

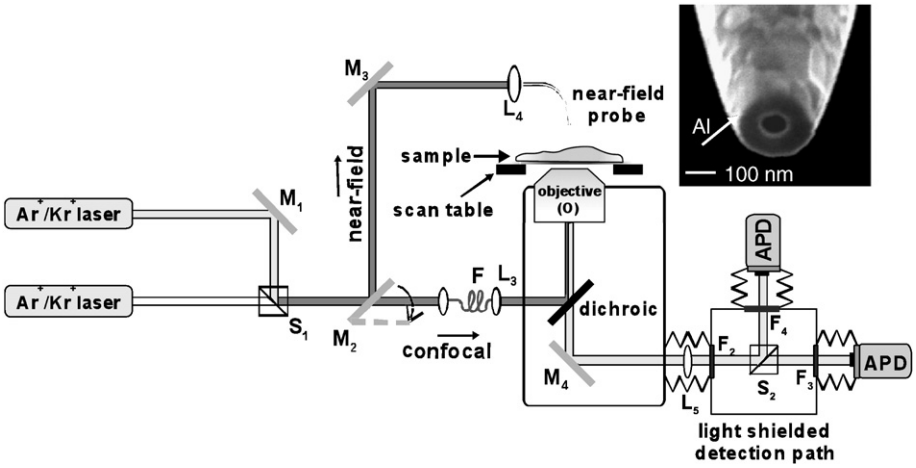

Fig. 3. Schematics of our combined confocal/NSOM set-up. Two laser lines can be simultaneously coupled into the microscope using the confocal or NSOM excitation configuration modes. Easy switching from one mode of excitation or the other is achieved by a flipable mirror (M_2 in the scheme). Fluorescence light is collected using a high NA objective and selected using appropriate filters. The fluorescence signal is then separated according to polarization (using a polarizing beam splitter) or spectral (using a dichroic mirror) properties (S_2 in the scheme) and sent to two sensitive detectors (APDs). The inset shows a 70-nm diameter NSOM probe. The aperture primarily determines the optical resolution of the microscope.

or the probe. In the case of the scanner locked to the specimen, which is the most employed configuration for biological imaging, the sample is moved in a raster pattern. The image is generated from the signal arising from the tip–specimen interaction under the probe, which is fixed and aligned confocally to the objective. The size of the area imaged depends uniquely on the coarse of the scanner. During raster scanning, data obtained both from the feedback system and from the optical detectors are simultaneously stored by a computer point by point. Finally, the PC compiles and renders the acquired data and furnishes simultaneously topography and optical image of the specimen.

One of the major obstacles that have restricted the use of NSOM in cell biology has been related to its difficulty to operate in liquid conditions, a crucial step towards live cell imaging. Successful control of the tip–sample distance has been routinely achieved in air by using tuning forks as sensing elements and driven at resonance [77,78]. However, this approach systematically failed once the tuning fork was immersed in a liquid. Koopman et al have demonstrated that, in aqueous environments, sensitivity of the surface topography can be regained by keeping the tuning fork dry in a "diving bell" enclosure just above the probe [86,87]. Alternatively Höppener and colleagues used the tuning fork with the tip placed perpendicular to the prongs of the fork and protruding about ~2 mm below the fork. The configuration works thus as "tapping-mode" with the tip immerse in solution and the tuning fork kept dry above the liquid [88]. An alternative method for position control is based on ion conductance. The method relies on the use of sharp micropipettes. As the probe approaches the sample, ion conduction is partially blocked and the change in conductivity is used as a measure of the tip–sample distance [89]. This mechanism has been coupled to NSOM to obtain images in living cells [89].

Although NSOM provides nanometric optical resolution together with simultaneous topographic information using a multitude of different optical contrast mechanisms, one should also be aware of the current limitations of the technique. For instance, NSOM is prone to artifacts generated from the topographic signal used to control the separation between the tip and sample. Therefore relatively flat samples (with height differences below 1 μm) are preferred for imaging. As scanning technique, NSOM is inherently slow, and thus not suitable for recording fast dynamic processes in living cells. On the other hand, recent developments on NSOM combined with FCS might provide truly dynamic information at the nanometer scale [90]. Finally, aperture probes have low throughput efficiencies (typically 10^{-4}–10^{-6}), limiting the number of photons that can be forced out the tip. Current developments using optical nanoantennas to concentrate and enhance the electric field at the antenna end hold great promise for the use of these engineered probes in bioimaging [91].

5. Probing model and cell membrane architectures with near-field optical microscopy

5.1. Model membranes inspected by NSOM

Model membranes have been used for a long time to investigate the segregation behavior of lipids and different proteins in predetermined lipid mixtures, while reducing the complexity of the cell membrane. The typical binary or ternary lipid mixtures used to mimic the lipid composition of cell membranes indeed phase-segregate into liquid condensed (LC) and liquid expanded (LE) phases. By transferring monolayers of a lipid mixture on a substrate using standard Langmuir-Blodgett techniques, Hwang et al. used NSOM to reveal previously unresolved features of around 50 nm [92,93]. When a higher pressure was used to form the monolayer, the domains of LC phase appeared to decrease in size and an increasingly complex fine web structure of the LE phase emerged [92,93]. Cholesterol addition, typically enriching the LC phase, resulted in the formation of elongated thin LC domains. From these morphology changes it was concluded that cholesterol reduced the line tension between the domains in regions of LC/LE coexistence. Likewise, the addition of the ganglioside GM1, again a LC constituent, affected the monolayer morphology significantly. Moreover, GM1 induced a more pronounced segregation between the LC and LE phases. These results suggested the formation of genuine distinct domains, thus favoring the occurrence of a lipid raft type of phenomenon on model membranes. The lipids typically enriching the LC phase are significantly more saturated than lipids constituting the LE phase. Thus, when all lipids pack in their subsequent phase, the LE phase will be lower in height. Indeed, by specifically labeling the LE phase a perfect correlation was found between topographical and fluorescence signals [94]. To extend these findings, Hollars and Dunn used tapping-mode feedback NSOM to additionally obtain compliance information of the lipid monolayer [95]. Because the carbohydrate chains of the lipids from the LC phase are highly saturated they pack in an ordered fashion as compared to the lipids from the LE phase. As expected, the LC phase was found less compliant than the LE phase [95]. As such Hollars and Dunn demonstrated the strength of NSOM as compared to fluorescence or scanning probe techniques on their own.

In a more recent work supporting the formation of lipid rafts on model membranes, small amounts of labeled GM1 revealed that GM1 is not homogeneously distributed throughout the LC phase. Instead, they were seen to constitute their own 100–200 nm sized domains [96]. In fact, upon closer examination the labeled GM1 distribution appeared to be more complex. To better characterize the GM1 behavior, GM1 lipids were labeled with Bodipy. This fluorophore displays a redshift in the emission spectra when present in higher concentrations due to excimer formation, thus being able to probe the local lipid density [97]. Due to the strong tendency of GM1 to partition in gel or liquid-ordered phases high concentration GM1 was found in the LC phase, showing the redshifted emission, even while using low deposition pressures [98]. Nevertheless, a rather large fraction of single Bodipy-GM1 was still found randomly distributed in the LE phase. Upon increasing the deposition pressure towards expected cell membrane pressures, the LC domain phases became smaller and the labeled GM1 appeared to preferentially partition into the LC phase [98].

The use of NSOM to investigate monolayers has been extended towards bilayers [99] and protein containing lipid layers [88,100–102]. The addition of proteins to such lipid phase-segregated model systems will be an important step in understanding how lipid based interaction can influence protein distribution. Subsequently, monitoring the dynamics would then provide a more complete spatio-temporal map of proteins and lipids in a lipid bilayer. Work in this direction has been performed using atomic force microscopy in combination with FCS [103]. The recent proof-of-principle indication that dynamical studies can be also performed with NSOM [90] opens up an exciting field that combines high-resolution imaging with ultrafast dynamics. Indeed, the advantage of performing FCS on confined volumes has been recently demonstrated on living cells [54,104]. The incorporation of this approach in NSOM would provide in addition to surface sensitivity, topography and resolution, also temporal information.

5.2. Cell membrane compartmentalization inspected by NSOM

Within cell membrane quantitative imaging, NSOM has been mainly used to investigate the degree of clustering of different receptors on the cell membrane. In some cases, the association of multiple components has been also investigated using dual color NSOM. In the context of receptor clustering our group has used NSOM to image pathogen recognition receptors with high spatial resolution on cells of the immune system, providing insight into the mechanisms exploited by the cell to ensure high performance of these receptors [87,105–107] (Fig. 4). By labeling the pathogen recognition receptor DC-SIGN with a specific monoclonal antibody, we found that as much as 80% of DC-SIGN is clustered on the cell membrane of immature dendritic cells [107]. These domains were randomly distributed over the plasma membrane with a size distribution centered ~185 nm. Interestingly, we discovered a remarkable heterogeneity of the DC-SIGN packing density within the clusters. This suggests that the large spread in DC-SIGN density per cluster likely serves to maximize the chances of DC-SIGN binding to a large variety of viruses and pathogens having different binding affinities [107]. Indeed, the organization of DC-SIGN in nanodomains appeared crucial for efficient binding and internalization of pathogens [15].

Recently, Chen et al. used NSOM in combination with quantum dots to label the T cell receptor (TCR) of T cells in live animals before and after cell stimulation [108]. In the resting state, the TCR complexes were found monomerically organized on the T cell membrane. Upon T cell stimulation, the TCR complexes reorganized and formed 270–390 nm sized domains. Interestingly, these small-sized domains were not only formed but also sustained for days. Additional experiments showed that although unstimulated cells could produce an immune response, stimulated cells produced

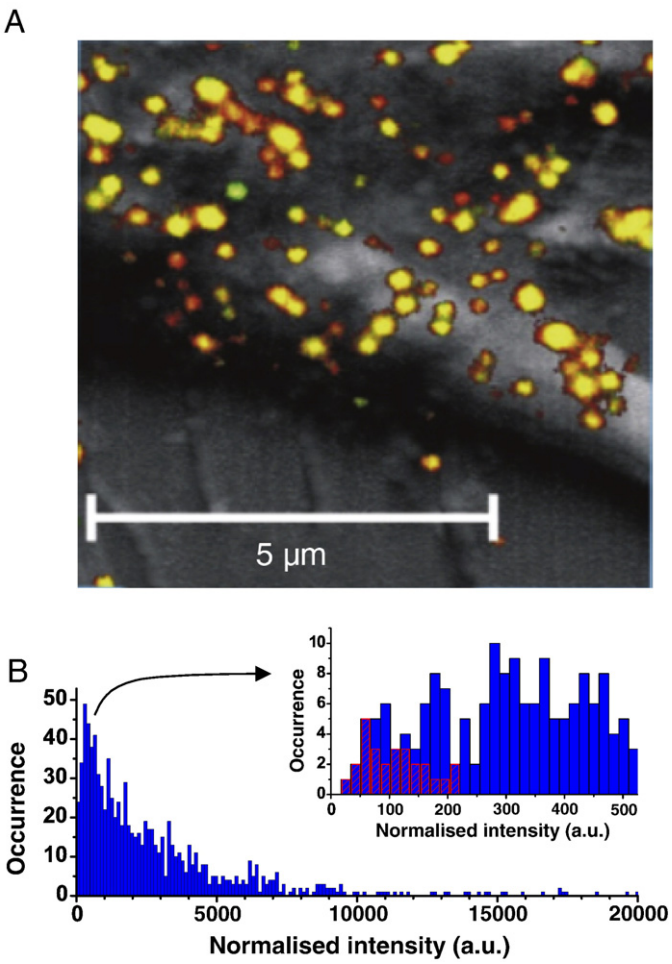

Fig. 4. Super-resolution image of a dendritic cell expressing the pathogen recognition receptor DC-SIGN. (A) Simultaneously obtained topography (gray) and NSOM fluorescence (color spots) on a small region of the dendritic cell surface. The color-coding reflects the emission dipole moment of individual molecules on the cell membrane, with red and green spots corresponding to different molecular in-plane orientations. Most of the spots are yellow and have different physical sizes, a clear signature for clustering of DC-SIGN. (B) Intensity brightness distribution over 1200 different spots from multiple NSOM images. The long tail of the distribution reflects the diverse clustering exhibited by DC-SIGN. The inset shows the expanded intensity axis and superposed to it, the brightness distribution of individual Cy5 molecules (red bars).

significant higher levels of cytokines [108]. By means of these high-resolution NSOM experiments it was shown that the TCR reorganization plays a significant role in antigen recognition and cytokine production.

In the case of members of the epidermal growth factor (EGF) receptor tyrosine kinase family, clustering is thought to have a negative effect. Some EGFs, like the erbB2 receptor, are found to be over-expressed in breast cancerous cells. It is thought that this over-expression leads to cluster formation causing the highly oncogenic activation of very potent kinase activity. Indeed, by applying NSOM the clustering behavior of EGF receptors was found to be associated with the activation state of the cell [109]. Additionally, it was found that EGF cluster sizes increased if the quiescent cells were treated with EGF activators to the same extend as cells over-expressing these EGFs [109]. Since activation of the EGF signaling pathways requires extensive interaction between individual members of the EGF family, it is likely that concentrating one of these EGF receptors in clusters increases the likelihood of co-clustering of other EGF members. This co-clustering would then subsequently increase the EGF signaling efficiency. In other words, a higher local concentration will decrease the lag time for direct inter-receptor contact.

Cell signaling events commonly involve a multitude of spatially segregated proteins and lipids. As such, standard confocal microscopy studies in biology usually involve multiple colors corresponding to multiple specifically labeled proteins. However, inherent to all lens-based techniques are chromatic aberrations that cause multiple wavelengths to never perfectly overlap. In contrast, NSOM guarantees a perfect overlay between multiple excitation wavelengths, an essential requirement to resolve the true nanoscale landscape of cell membranes. Already in 1997, Enderle et al. used for the first time dual-color NSOM to directly measure the association of a host protein (protein4.1) and parasite proteins (MESA and PfHRP1) in malaria (*Plasmodium falciparum*) infected erythrocytes [110]. As the parasitic proteins interact with the host proteins, 100 nm sized knob-like topographical features appear on the membrane of the host cell. To investigate the direct interaction of host and parasite proteins, the proteins were specifically labeled and subsequently imaged with NSOM. As expected, the fluorescence from the two labeled parasitic proteins and the labeled host protein were found on the knob like structures. However, this did not necessarily involve colocalization of host and parasite proteins [110].

The increased co-localization of individual components on the cell membrane has been actually demonstrated on two members of the interleukin family by combining dual-color excitation and single molecule detection NSOM [111]. IL2R and IL15R did not interact if their organization was monomeric. However, in their clustered form, both receptors were found to co-localize significantly suggesting that clustering of both receptors takes place in the same nanocompartments [111]. Interestingly, IL2R and IL15R clusters were found to have a constant packing density albeit forming domains of different sizes [111]. Although the receptors were found to pack at different densities, the linear increase in number of receptors with domain size suggested a general *building block* type of assembly for these receptors [111].

Ianoul et al. have also used dual-color NSOM to investigate the association of β-adrenergic receptors (βAR) and caveolae of the surface of cardiac myocytes [112]. The study showed that ~15–20% β_2ARs colocalize in caveolae. The lack of complete colocalization of β_2AR with the caveolae suggested that the diverse functional properties of the β_2AR could arise from its association with multi-protein complexes of different compositions that may not be caveolar in nature. Interestingly, the fraction of β_2ARs not colocalizing with caveolae appeared proximal to it, indicating β_2AR complexes are pre-assembled in, or near caveolae. More conventionally used techniques such as FRET are unable to report on such a proximity effect at spatial scales >10 nm. On the other extreme, diffraction limited techniques such as confocal microscopy will not be able to reveal a lack of co-localization if multiple components are located at distances <300 nm. As such, NSOM is capable of bridging the gap between 10 to 300 nm providing valuable information at these important spatial scales.

Fig. 5 shows as example the powerfulness of dual color excitation and detection NSOM when imaging two different components of the cell membrane. The high packing density of both components on the cell surface combined with the limited resolution of confocal microscopy suggests colocalization between GM1 nanoclusters and the receptor DC71. However, high-resolution NSOM shows clearly that these receptors do not compartmentalize in the same regions of the cell membrane.

More recently, NSOM has been also used to spatially relate topographical features to two different lipid species [113]. Both GM1 and GM3 were seen to cluster in 40–360 nm domains that distributed randomly on the plasma membrane of epithelial cells. However, upon closer examination it appeared that the GM3 clusters were localized on the peaks of microvillus-like structures [113]. In contrast, the majority of the GM1 lipid clusters were found in the valley or slopes of these topographical protrusions [113]. These results highlight the importance of correlating topography and optical information uniquely afforded by NSOM. Along these lines, it is worthy to mention that several groups have also implemented AFM in combination with confocal microscopy in order to correlate topography with fluorescence information, albeit at lower optical resolution (diffraction-limited). On the other hand, a combination of AFM and confocal FCS can also provide complementary information on the dynamics of different nanoenviroments on membranes and correlate it with topographic information as afforded by AFM [103].

6. Summary and outlook

In summary, the past few years have witnessed tremendous technical advances in super-resolution optical microscopy using both far and near-field methods. This has in turn further increased our understanding on the compartmentalization of the cell membrane and its implications in cellular function and diseases. However, a significant number of questions are still open and awaiting for techniques that combine high spatial and temporal resolution in one and the same instrument. Far-field super-resolution methods have already demonstrated the possibility of following the dynamics of slowly moving receptors on the cell membrane on small fields of views [53,63–65] or in combination with a FCS approach [54]. Further developments of probes and instrumentation will certainly lead to improvement of these techniques.

Within the context of near-field super-resolution, first demonstrations of NSOM measurements on living cells have been reported [114–116] although high-resolution dynamics on the membrane of living cells is yet to be demonstrated. Obviously, if the scanning speed

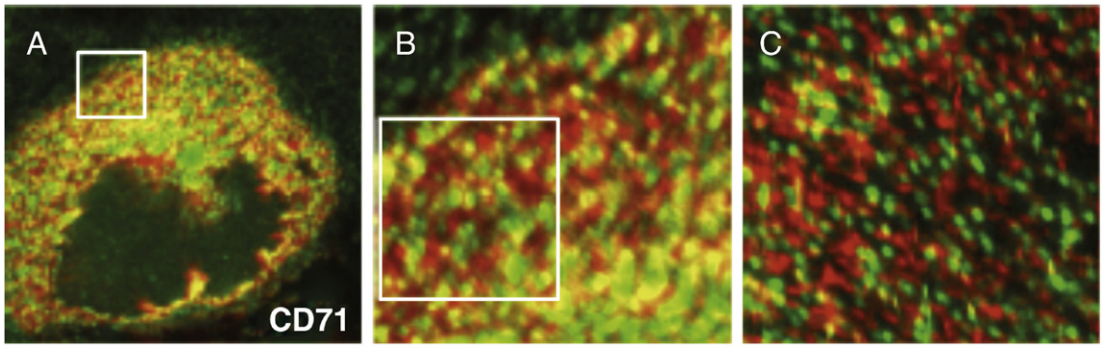

Fig. 5. Dual color super-resolution NSOM in aqueous conditions of different membrane components. (A) Representative confocal fluorescence image taken at the focal plane of the glass surface of a monocytic cell showing the merging of the lipid GM1 (labeled with CTxB, red) and the receptor CD71 (labeled with specific antibodies, green) (40×40 μm^2). An area of interest, as indicated by the white box is further inspected by confocal microscopy in (B) (10×10 μm^2). Multiple yellow patches in the confocal image suggest colocalization between GM1 and CD71. (C) NSOM image of the highlighted area in B, obtained after excitation using a probe of ~100 nm in diameter (5×5 μm^2). The apparent colocalization observed in confocal disappears upon high-resolution inspection afforded by NSOM (physically separated red and green spots) indicating that CD71 does not colocalize with GM1, entirely consistent with its assignment as non-raft marker.

is not significantly faster than protein diffusion the optical signal will be blurred. Nevertheless, the promising demonstration of subwavelength FCS [90] opens the way for probing dynamics at relevant spatial scales potentially revealing the driving mechanisms for nanodomain formation and evolution during cell activation. Additionally, multicolor cross-correlation should indicate if certain proteins are diffusing in identical or separate domains. The combination of capabilities that is offered by NSOM makes the technique a worthy and essential asset in the spectra of biophysical techniques available nowadays.

Acknowledgments

The workers thank B. I de Bakker and M. Koopman for some of the images shown and part of the written material discussed in this review. This work was supported by grants from the NWO Veni grant 916.66.028 and the Human Frontiers program (to AC), EC-RTN-IMMUNANOMAP and EC-NEST-BIO-LIGHT-TOUCH (to MFG-P and TvZ).

References

[1] S.J. Singer, G.L. Nicolson, The fluid mosaic model of the structure of cell membranes, Science 175 (1972) 720–731.
[2] K. Jacobson, E.D. Sheets, R. Simon, Revisiting the fluid mosaic model of membranes, Science 268 (1995) 1441–1442.
[3] F.R. Maxfield, Plasma membrane microdomains, Curr. Opin. Cell Biol. 14 (2002) 483–487.
[4] Y. Chen, B.C. Lagerholm, B. Yang, K. Jacobson, Methods to measure the lateral diffusion of membrane lipids and proteins, Methods 39 (2006) 147–153.
[5] K. Jacobson, O.G. Mouritsen, R.G.W. Anderson, Lipid rafts: at a crossroad between cell biology and physics, Nat. Cell Biol. 9 (2007) 7–14.
[6] C.A. Day, A.K. Kenworthy, Tracking microdomains in cells membranes, Biochim. Biophys. Acta 1788 (2009) 245–253.
[7] S. Chiantia, J. Ries, P. Schwille, Fluorescence correlation spectroscopy in membrane structure elucidation, Biochim. Biophys. Acta 1788 (2009) 225–233.
[8] M. Edidin, Lipids on the frontier: a century of cell membrane bilayers, Nat. Rev. Mol. Cell Bio. 4 (2003) 414–418.
[9] A.K. Kenworthy, B.J. Nichols, C.L. Remmert, G.M. Hendrix, M. Kumar, J. Zimmerberg, J. Lippincott-Schawartz, Dynamics of putative raft-associated proteins at the cell surface, J. Cell Bio. 165 (2004) 735–746.
[10] S. Mayor, M. Rao, Rafts: scale-dependent, active lipid organization at the cell surface, Traffic 5 (2004) 231–240.
[11] J.F. Hancock, Lipid rafts: contentious only from simplistic standpoints, Nat. Rev. Mol. Cell Bio. 7 (2006) 456–462.
[12] B. Razani, S.E. Woodman, M.P. Lisanti, Caveolae: from cell biology to animal physiology, Pharmacol. Rev 54 (2002) 431–467.
[13] L.J. Pike, Rafts defined: a report on the Keystone symposium on lipid rafts and cell function, J. Lipid Res. 47 (2006) 1597–1598.
[14] A. Cambi, B. Joosten, M. Koopman, F. de Lange, I. Beeren, R. Torensma, J.A. Fransen, M. Garcia-Parajo, F.N. van Leeuwen, C.G. Figdor, Organization of the integrin LFA-1 in nanoclusters regulates its activity, Mol. Bio. Cell 17 (2006) 4270–4281.
[15] A. Cambi, F. de Lange, N.M. van Maarseveen, M. Nijhuis, B. Joosten, E.M. van Dijk, B.I. de Bakker, J.A. Fransen, P.H. Bovee-Geurts, F.N. van Leeuwen, N.F. van Hulst, C.G. Figdor, Microdomains of the C-type lectin DC-SIGN are portals for virus entry into dendritic cells, J. Cell Bio. 164 (2004) 145–155.
[16] S. Mayor, R.E. Pagano, Pathways of clathrin-independent endocytosis, Nat Rev. Mol. Cell Bio. 8 (2007) 603–612.
[17] S. Manes, A. Viola, Lipid rafts in lymphocyte activation and migration, Mol. Mem. Biol. 23 (2006) 59–69.
[18] T. Suzuki, Y. Suzuki, Virus infection and lipid rafts, Biol. Pharma. Bull. 29 (2006) 1538–1541.
[19] V. Michel, M. Bakovic, Lipid rafts in health and disease, Biol. Cell 99 (2007) 129–140.
[20] C.R. Bollinger, V. Teichgraber, E. Gulbins, Ceramide-enriched membrane domains, Biochim. Biophys. Acta 1746 (2005) 284–294.
[21] P. Sharma, R. Varma, R.C. Sarasij, K. Ira, G. Gousset, M. Krishnamoorthy, S. Rao, Mayor, Nanoscale organization of multiple GPI-anchored proteins in living cell membranes, Cell 116 (2004) 577–589.
[22] D. Goswami, K. Gowrishankar, S. Bilgrami, S. Ghosh, R. Raghupathy, R. Chadda, R. Vishwakarma, M. Rao, S. Mayor, Nanoclusters of GPI-anchored proteins are formed by cortical actin-driven activity, Cell 135 (2008) 1085–1097.
[23] R. Lasserre, X.J. Guo, F. Conchonaud, Y. Hamon, O. Hawchar, A.M. Bernard, S.M. Soudja, P.F. Lenne, H. Rigneault, D. Olive, G. Bismuth, J.A. Nunes, B. Payrastre, D. Marguet, H.T. He, Raft nanodomains contribute to Akt/PKB plasma membrane recruitment and activation, Nat. Chem. Bio. 4 (2008) 538–547.
[24] M. Wu, D. Holowka, H.G. Craighead, B. Baird, Visualization of plasma membrane compartmentalization with patterned lipid bilayers, Proc. Natl. Acad. Sci. USA 101 (2004) 13798–13803.
[25] S. Munro, An investigation of the role of transmembrane domains in Golgi protein retention, EMBO J. 14 (1995) 4695–4704.
[26] R. Fragoso, D. Ren, X. Zhang, M.W. Su, S.J. Burakoff, Y.J. Jin, Lipid raft distribution of CD4 depends on its palmitoylation and association with Lck, and evidence for CD4-induced lipid raft aggregation as an additional mechanism to enhance CD3 signaling, J. Immunol. 170 (2003) 913–921.
[27] M. Yamabhai, R.G. Anderson, Second cysteine-rich region of epidermal growth factor receptor contains targeting information for caveolae/rafts, J. Bio. Chem. 277 (2002) 24843–24846.
[28] A. Cherukuri, R.H. Carter, S. Brooks, W. Bornmann, R. Finn, C.S. Dowd, S.K. Pierce, B cell signaling is regulated by induced palmitoylation of CD81, J. Bio. Chem. 279 (2004) 31973–31982.
[29] A.D. Douglass, R.D. Vale, Single-molecule microscopy reveals plasma membrane microdomains created by protein-protein networks that exclude or trap signaling molecules in T cells, Cell 121 (2005) 937–950.
[30] S. Charrin, S. Manie, M. Billard, L. Ashman, D. Gerlier, C. Boucheix, E. Rubinstein, Multiple levels of interactions within the tetraspanin web, Biochem. Biophys. Res. Commun. 304 (2003) 107–112.
[31] C. Espenel, E. Margeat, P. Dosset, C. Arduise, C. Le Grimellec, C.A. Royer, C. Boucheix, E. Rubinstein, P.E. Milhiet, Single-molecule analysis of CD9 dynamics and partitioning reveals multiple modes of interaction in the tetraspanin web, J. Cell Bio. 182 (2008) 765–776.
[32] F. Berditchevski, Complexes of tetraspanins with integrins: more than meets the eye, J. Cell Sci. 114 (2001) 4143–4151.
[33] J. Lammerding, A.R. Kazarov, H. Huang, R.T. Lee, M.E. Hemler, Tetraspanin CD151 regulates alpha6beta1 integrin adhesion strengthening, Proc. Natl. Acad. Sci. USA 100 (2003) 7616–7621.
[34] C. Dietrich, B. Yang, T. Fujiwara, A. Kusumi, K. Jacobson, Relationship of lipid rafts to transient confinement zones detected by single particle tracking, Biophys. J. 82 (2002) 274–284.
[35] A. Viola, N. Gupta, Tether and trap: regulation of membrane-raft dynamics by actin-binding proteins, Nat. Rev. Immunol. 7 (2007) 889–896.
[36] T. Fujiwara, K. Ritchie, H. Murakoshi, K. Jacobson, A. Kusumi, Phospholipids undergo hop diffusion in compartmentalized cell membrane, J. Cell Bio. 157 (2002) 1071–1081.
[37] A. Kusumi, C. Nakada, K. Ritchie, K. Murase, K. Suzuki, H. Murakoshi, R.S. Kasai, J. Kondo, T. Fujiwara, Paradigm shift of the plasma membrane concept from the two-dimensional continuum fluid to the partitioned fluid: high-speed single-molecule tracking of membrane molecules, Annu. Rev. Biophys. Biomol. Struct. 34 (2005) 351–378.
[38] P.F. Lenne, L. Wawrezinieck, F. Conchonaud, O. Wurtz, A. Boned, X.J. Guo, H. Rigneault, H.T. He, D. Marguet, Dynamic molecular confinement in the plasma membrane by microdomains and the cytoskeleton meshwork, EMBO J. 25 (2006) 3245–3256.
[39] N.L. Andrews, K.A. Lidke, J.R. Pfeiffer, A.R. Burns, B.S. Wilson, J.M. Oliver, D.S. Lidke, Actin restricts FcεRI diffusion and facilitates antigen-induced receptor immobilization, Nat. Cell Bio. 10 (2008) 955–963.
[40] M. Saxton, K. Jacobson, Single particle tracking: applications to membrane dynamics, Annu. Rev. Biophys. Biomol. Struct. 26 (1997) 373–399.
[41] A. Kenworthy, Imaging protein-protein interactions using fluorescence resonance energy transfer microscopy, Methods 24 (2001) 289–296.
[42] O.O. Glebov, B.J. Nichols, Lipid raft proteins have a random distribution during localized activation of the T-cell receptor, Nat. Cell. Bio. 6 (2004) 238–243.
[43] L.M.S. Loura, R.F.M. de Almeida, L.C. Silva, M. Pietro, FRET analysis of domain formation and properties in complex membrane systems, Biochim. Biophys. Acta 1788 (2009) 209–224.
[44] B. Wilson, S. Steinberg, K. Liederman, J. Pfeiffer, Z. Surviladze, J. Zhnag, L. Samelson, L. Yang, P. Kotula, J. Oliver, Markers for detergent-resistant lipid rafts occupy distinct and dynamic domains in native membranes, Mol. Bio. Cell 15 (2004) 2580–2592.
[45] S.T. Hess, M. Kumar, A. Verma, J. Farrington, A. Kenworthy, J. Zimmerberg, Quantitative electron microscopy and fluorescence spectroscopy of the membrane distribution of influenza hemagglutitin, J. Cell Bio. 169 (2005) 965–976.
[46] I. Prior, C. Muncke, R. Parton, J. Hancock, Direct visualization of Ras proteins in spatially distinct cell surface microdomains, J. Cell Bio. 160 (2003) 165–170.
[47] S.J. Plowman, C. Muncke, R. Parton, J. Hancock, H-ras, K-ras, and inner plasma raft proteins operate in nanoclusters with differential dependence on the actin cytoskeleton, Proc. Natl. Acad. Sci. USA. 102 (2005) 15500–15505.
[48] V. Westphal, S.W. Hell, Nanoscale resolution in the focal plane of an optical microscope, Phys. Rev. Lett. 94 (2005) 143903.
[49] G. Donnert, J. Keller, R. Medda, M.A. Andrei, S.O. Rizzoli, R. Luhrmann, R. Jahn, C. Eggeling, S.W. Hell, Macromolecular-scale resolution in biological fluorescence microscopy, Proc. Natl. Acad. Sci. USA 103 (2006) 11440–11445.
[50] K.I. Willig, S.O. Rizzoli, V. Wesphal, R. Jahn, S.W. Hell, STED microscopy reveals hat synaptotagmin remains clustered after synpatic vesicle exocytosis, Nature 440 (2006) 935–939.
[51] J.J. Sieber, K.I. Willig, C. Kutzner, C. Gerding-Reimers, B. Harke, G. Donnert, B. Rammner, C. Eggeling, S.W. Hell, H. Grubmuller, T. Lang, Anatomy and dynamics of a supramolecular membrane protein cluster, Science 317 (2007) 1072–1076.
[52] R.R. Kellner, C.J. Baier, K.I. Willig, S.W. Hell, F.J. Barrantes, Nanoscale organization of nicotinic acetylcholine receptors revealed by stimulated emission depletion microscopy, Neuroscience 144 (2007) 135–143.
[53] V. Wesphal, S.O. Rizzoli, M.A. Lauterbach, D. Kamin, R. Jahn, S.W. Hell, Video-rate far-field optical nanoscopy dissects synaptic vesicle movement, Science 320 (2008) 246–249.
[54] C. Eggeling, C. Ringemann, R. Medda, G. Schwarzmann, K. Sandhoff, S. Polyakova, V.N. Belov, B. Hein, C. von Middendorff, A. Schonle, S.W. Hell, Direct observation

of the nanoscale dynamics of membrane lipids in a living cell, Nature 457 (2009) 1159–1162.
[55] M.G.L. Gustafsson, Non-linear structured-illumination microscopy: wide-field fluorescence imaging with theoretically unlimited resolution, Proc. Natl. Acad. Sci. USA 102 (2005) 13081–13086.
[56] L. Schermelleh, P.M. Carlton, S. Haase, L. Shao, L. Winoto, P. Kner, B. Burke, M.C. Cardoso, D.A. Agard, M.G.L. Gustafsson, H. Leonhardt, J.W. Sedat, Subdiffraction multicolor imaging of the nuclear periphery with 3D structured illumination microscopy, Science 320 (2008) 1332–1336.
[57] M.G.L. Gustaffson, L. Shao, P.M. Carlton, C.J.R. Wang, I.N. Golubovskaya, W.Z. Cande, D.A. Agard, J.W. Sedat, Three-dimensional resolution doubling in wide-field fluorescence microscopy by structured illumination, Biophys. J. 94 (2008) 4957–4970.
[58] J. Pielage, L. Cheng, R.D. Fetter, P.M. Carlton, J.W. Sedat, G.W. Davis, A presynaptic giant ankrin stabilizes the NMJ through regulation of presynaptics microtubules and transsynaptic cell adehesion, Neuron 58 (2008) 195–209.
[59] E. Betzig, G.H. Patterson, R. Sougrat, O.W. Lindwasser, S. Olenuch, J.S. Bonifacino, M.W. Davidson, J. Lippincott-Schwartz, H.F. Hess, Imaging intracellular fluorescent proteins at nanometer resolution, Science 313 (2006) 1642–1645.
[60] S.T. Hess, T.P.K. Girirajan, M.D. Mason, Ultra-high resolution imaging by fluorescence photoactivation localization microscopy, Biophys. J. 91 (2006) 4258–4272.
[61] M.J. Rust, M. Bates, X. Zhuang, Subdiffraction limit imaging by stochastic optical reconstruction microscopy (STORM), Nat. Methods 3 (2006) 793–796.
[62] H. Schroff, C.G. Galbraith, J.A. Galbraith, H. White, J. Gillete, S. Olenych, M.W. Davidson, E. Betzig, Dual-color super-resolution imaging of genetically expressed probes within adhesion complexes, Proc. Natl. Acad. Sci. USA 104 (2007) 20308–20313.
[63] S. Manley, J.M. Gillete, G.H. Patterson, H. Schroff, H.F. Hess, E. Betzig, J. Lippincott-Schwartz, High-density mapping of single molecule trajectories with photo-activated localization microscopy, Nat. Methods 5 (2008) 155–157.
[64] S.T. Hess, T.J. Gould, M.V. Gudheti, S.A. Maas, K.D. Mills, J. Zimmerberg, Dynamic clustered distribution of hemagglutinin resolved at 40 nm in living cell membranes discriminates between raft theories, Proc. Natl. Acad. Sci. USA 104 (2007) 17370–17375.
[65] H. Schroff, C.G. Galbraith, J.A. Galbraith, E. Betzig, Live cell photoactivated localization microscopy of nanoscale adhesion dynamics, Nat. Methods 5 (2008) 417–423.
[66] M. Bates, B. Huang, G.T. Dempsey, X. Zhuang, Multicolor super-resolution imaging with photo-switchable fluorescent probes, Science 317 (2007) 1749–1753.
[67] B. Huang, W. Wang, M. Bates, X. Zhuang, Three-dimensional super-resolution imaging by stochastic optical reconstruction microscopy, Science 319 (2008) 810–813.
[68] M.F. Juette, T.J. Gould, M.D. Lessard, M.J. Mlodzianoski, B.S. Nagpure, B.T. Bennett, S.T. Hess, J. Bewersdorf, Three-dimensional sub-100 nm resolution fluorescence microscopy in thick samples, Nat. Methods 5 (2008) 527–529.
[69] S.R.P. Pavani, M.A. Thompson, J.S. Biteen, S.J. Lord, N. Liu, R.J. Twieg, R. Piestun, W.E. Moerner, Three-dimensional, single-molecule fluorescence imaging beyond the diffraction limit by using a double helix point spread function, Proc. Natl. Acad. Sci. USA 106 (2009) 2995–2999.
[70] G. Shtengel, J.A. Galbraith, C.G. Galbraith, J. Lippincott-Scharwartz, J.M. Gillete, S. Manley, R. Sougrat, C.M. Waterman, P. Kanchanawong, M.W. Davidson, R.D. Fetter, H.F. Hess, Interferometric fluorescent super-resolution microscopy resolves 3D cellular ultrastructure, Proc. Natl. Acad. Sci. USA 106 (2009) 3125–3130.
[71] J. Lippincott-Schwartz, S. Manley, Putting super-resolution fluorescence microscopy to work, Nat. Methods 6 (2009) 21–23.
[72] N. Ji, H. Shroff, H. Zhong, E. Betzig, Advances in the speed and resolution of light microscopy, Curr. Opin. Neurobio. 18 (2008) 605–616.
[73] D.W. Pohl, W. Denk, M. Lanz, Optical stethoscopy: image recording with resolution $\lambda/20$, Appl. Phys. Lett. 44 (1984) 651–653.
[74] E. Betzig, J.K. Trautman, T.D. Harris, J.S. Weiner, R.L. Kostelak, Breaking the diffraction barrier: optical microscopy on a nanometric scale, Science 251 (1991) 1468–1470.
[75] N.F. van Hulst, M.F. Garcia-Parajo, M.H.P. Moers, J.A. Veerman, A.G.T. Ruiter, Near-field fluorescence imaging of genetic material: towards the molecular limit, J. Struct. Bio. 119 (1997) 222–231.
[76] B. Hecht, B. Sick, U.P. Wild, V. Deckert, R. Zenobi, O.J.F. Martin, D.W. Dieter, Scanning near-field optical microscopy with aperture probes: fundamentals and applications, J. Chem. Phys. 112 (2000) 7761–7774.
[77] K. Karrai, R.D. Grober, Piezo-electric tip-sample distance control for near field optical microscopes, Appl. Phys. Lett. 66 (1995) 1842–1844.
[78] A.G. Ruiter, J.A. Veerman, K.O. van der Werf, N.F. van Hulst, Dynamic behavior of tuning fork shear-force feedback, Appl. Phys. Lett. 71 (1997) 28–30.
[79] M.L.M. Balistreri, H. Gersen, J.P. Korterik, L. Kuipers, N.F. van Hulst, Tracking femtosecond laser pulses in space and time, Science 294 (2001) 1080–1082.
[80] F. Zenhausern, Y. Martin, H.K. Wickramasinghe, Scanning interferometric apertureless microscopy: optical imaging at 10 Angstrom resolution, Science 269 (1995) 1083–1085.
[81] L. Novotny, S.J. Stranick, Near-field optical microscopy and spectroscopy with pointed probes, Annu. Rev. Phys. Chem. 57 (2006) 303–331.
[82] E.J. Sanchez, L. Novotny, X. Sunney-Xie, Near-field fluorescence microscopy based on two-photon excitation with metal tips, Phys. Rev. Lett. 82 (1999) 4014–4017.
[83] P. Anger, P. Bharadwaj, L. Novotny, Enhancement and quenching of single-molecule fluorescence, Phys. Rev. Lett. 96 (2006) 1130021–1130024.
[84] C. Höppener, L. Novotny, Antenna-based optical imaging of single Ca^{2+} transmembrane proteins in liquids, Nano Lett. 8 (2008) 642–646.
[85] C. Höppener, R. Beams, L. Novotny, Background suppression in near-field optical imaging, Nano Lett. 9 (2009) 903–908.
[86] M. Koopman, B.I. de Bakker, M.F. Garcia-Parajo, N.F. van Hulst, Shear force imaging of soft samples in liquid using a diving bell concept, Appl. Phys. Lett. 83 (2003) 5083–5085.
[87] M. Koopman, A. Cambi, B.I. de Bakker, B. Joosten, C.G. Figdor, N.F. van Hulst, M.F. Garcia-Parajo, Near-field scanning optical microscopy in liquid for high resolution single molecule detection on dendritic cells, FEBS Lett. 573 (2004) 6–10.
[88] C. Höppener, J.P. Siebrasse, R. Peters, U. Kubitscheck, A. Naber, High-resolution near-field optical imaging of single nuclear pore complexes under physiological conditions, Biophys. J. 88 (2005) 3681–3688.
[89] Y.E. Korchev, M. Raval, M.J. Lab, J. Gorelik, C.R.W. Edwards, T. Rayment, D. Klenerman, Hybrid scanning ion conductance and scanning near-field optical microscopy for the study of living cells, Biophys. J. 78 (2000) 2675–2679.
[90] D. Vobornik, D.S. Banks, Z. Lu, C. Fradin, R. Taylor, L.J. Johnston, Fluorescence correlation spectroscopy with sub-diffraction-limited resolution using near-field optical probes, Appl. Phys. Lett. 93 (2008) 163904–163906.
[91] M.F. Garcia-Parajo, Optical antennas focus in on biology, Nature Photonics 2 (2008) 201–203.
[92] J. Hwang, L.K. Tamm, C. Bohm, T.S. Ramalingam, E. Betzig, M. Edidin, Nanoscale complexity of phospholipid monolayers investigated by near-field scanning optical microscopy, Science 270 (1995) 610–614.
[93] J. Hwang, L.A. Gheber, L. Margolis, M. Edidin, Domains in cell plasma membranes investigated by near-field scanning optical microscopy, Biophys. J. 74 (1998) 2184–2190.
[94] C.W. Hollars, R.C. Dunn, Submicron structure in l-α-dipalmitoylphosphatidylcholine monolayers and bilayers probed with confocal, atomic force, and near-field microscopy, Biophys. J 75 (1998) 342–353.
[95] C.W. Hollars, R.C. Dunn, Submicron fluorescence, topography, and compliance measurements of phase-separated lipid monolayers using tapping-mode near-field scanning optical microscopy, J. Phys. Chem. B 101 (1997) 6313–6317.
[96] P. Burgos, C. Yuan, M.-L. Viriot, L.J. Johnston, Two-color near-field fluorescence microscopy studies of microdomains ("Rafts") in model membranes, Langmuir 19 (2003) 8002–8009.
[97] M. Dahim, N. Mizuno, X.M. Li, W.E. Momsen, M.M. Momsen, H.L. Brockman, Physical and photophysical characterization of a BODIPY phos-phatidylcholine as a membrane probe, Biophys. J. 83 (2002) 1511–1524.
[98] O. Coban, M. Burger, M. Laliberte, A. Ianoul, L.J. Johnston, Ganglioside partitioning and aggregation in phase-separated monolayers characterized by bodipy GM1 monomer/dimer emission, Langmuir 23 (2007) 6704–6711.
[99] A. Ianoul, P. Burgos, Z. Lu, R.S. Taylor, L.J. Johnston, Phase separation in supported phospholipid bilayers visualized by near-field scanning optical microscopy in aqueous solution, Langmuir 19 (2003) 9246–9254.
[100] B.N. Flanders, R.C. Dunn, A near-field microscopy study of submicron domain structure in a model lung surfactant monolayer, Ultramicroscopy 91 (2002) 245–251.
[101] R. Sibug-Aga, R.C. Dunn, High-resolution studies of lung surfactant collapse, Photochem. Photobiol. 80 (2004) 471–476.
[102] J. Murray, L. Cuccia, A. Ianoul, J. Cheetham, L.J. Johnston, Imaging the selective binding of synapsin to anionic membrane domains, Chembiochem 5 (2004) 1489–1494.
[103] S. Chiantia, N. Kahya, J. Ries, P. Schwille, Effects of ceramide on liquid-ordered domains investigated by simultaneous AFM and FCS, Biophys. J. 90 (2006) 4500–4508.
[104] J. Wenger, F. Conchonaud, J. Dintinger, L. Wawrezinieck, T.W. Ebbesen, H. Rigneault, D. Marguet, P.F. Lenne, Diffusion analysis within single nanometric apertures reveals the ultrafine cell membrane organization, Biophys. J. 92 (2007) 913–919.
[105] F. de Lange, A. Cambi, R. Huijbens, B.I de Bakker, W. Rensen, M.F. Garcia-Parajo, N.F. van Hulst, C.G. Figdor, Cell biology beyond the diffraction limit: near-field scanning optical microscopy, J. Cell Sci. 114 (2001) 4153–4160.
[106] M.F. Garcia-Parajo, B.I. de Bakker, M. Koopman, A. Cambi, F. de Lange, C.G. Figdor, N.F. van Hulst, Near-field fluorescence microscopy: an optical nanotool to study protein organization at the cell membrane, Nanobiotech. 1 (2005) 113–120.
[107] B.I. de Bakker, F. de Lange, A. Cambi, J.P. Korterik, E.M.H.P. van Dijk, N.F van Hulst, C.G. Figdor, M.F. Garcia-Parajo, Nanoscale organization of the pathogen receptor DC-SIGN mapped by single-molecule high-resolution fluorescence microscopy, Chemphyschem 8 (2007) 1473–1480.
[108] Y. Chen, L. Shao, Z. Ali, J. Cai, Z.W. Chen, NSOM/QD-based nanoscale immunofluorescence imaging of antigen-specific T-cell receptor responses during an in vivo clonal Vγ2Vδ2 T-cell expansion, Blood 111 (2008) 4220–4232.
[109] P. Nagy, A. Jenei, A.K. Kirsch, J. Sazollosi, S. Damjanovich, T.M. Jovin, Activation-dependent clustering of the erbB2 receptor tyrosine kinase detected by scanning near-field optical microscopy, J. Cell Sci. 112 (1999) 1733–1741.
[110] T. Enderle, T. Ha, D.F. Ogletree, D.S. Chemla, C. Magowan, S. Weiss, Membrane specific mapping and colocalization of malarial and host skeletal proteins in the *Plasmodium falciparum* infected erythrocyte by dual-color near-field scanning optical microscopy, Proc. Natl. Acad. Sci. USA 94 (1997) 520–525.
[111] B.I. de Bakker, A. Bodnar, E.P. van Dijk, G. Vámosi, S. Damjanovich, T.A. Waldmann, N.F. van Hulst, A. Jenei, M.F. Garcia-Parajo, Nanometer-scale organization of the alpha subunits of the receptors for IL2 and IL15 in human T lymphoma cells, J. Cell Sci. 121 (2008) 627–633.
[112] A. Ianoul, D.D. Grant, Y. Rouleau, M. Bani-Yaghoub, L.J. Johnston, J.P. Pezacki, Imaging nanometer domains of β-adrenergic receptor complexes on the surface of cardiac myocytes, Nat. Chem. Biol. 1 (2005) 196–202.

[113] Y. Chen, J. Qin, Z. Chen, Fluorescence-topographic NSOM directly visualizes peak-valley polarities of GM1/GM3 rafts in cell membrane fluctuations, J. Lipid Res. 49 (2008) 2268–2275.
[114] L.K. Kapkiai, D. Moore-Nichols, J. Carnell, J.R. Krogmeier, R.C. Dunn, Hybrid near-field scanning optical microscopy tips for live cell measurements, Appl. Phys. Lett. 84 (2004) 3750–3752.
[115] A. Ueda, O. Niwa, K. Maruyama, Y. Shindo, K. Oka, K. Suzuki, Neurite imaging of living PC12 cells with scanning electrochemical/near-field optical/atomic force microscopy, Angew. Chem. Int. Ed. Engl. 46 (2007) 8238–8241.
[116] G. Longo, M. Girasole, A. Cricenti, Implementation of a bimorph-based aperture tapping-SNOM with an incubator to study the evolution of cultured living cells, J. Microsc. 229 (2008) 433–439.